

## Cluster Compounds

## Confined Electron-Transfer Reactions within a Molecular Metal Oxide “Trojan Horse”\*\*

De-Liang Long, Hamera Abbas, Paul Kögerler, and Leroy Cronin\*

Dedicated to Professor Xin-Quan Xin on the occasion of his 70th birthday.

Heteropolyoxometalates (HPOMs) are molecular metal oxide clusters characterized by a vast structural diversity,<sup>[1]</sup> rich electrochemistry,<sup>[2]</sup> and versatile catalytic activities.<sup>[3]</sup> HPOMs frequently are derived from archetypal metal oxide cages of the general composition (MO<sub>3</sub>)<sub>x</sub> (M = Mo, W) that incorporate structurally vital tetrahedral anions (e.g., [SO<sub>4</sub>]<sup>2-</sup>, [PO<sub>4</sub>]<sup>3-</sup>, [SiO<sub>4</sub>]<sup>4-</sup>). Yet since the first structural elucidation of the archetypal Keggin HPOM [(MO<sub>3</sub>)<sub>12</sub>PO<sub>4</sub>]<sup>3-</sup> in 1933, and after many thousands of publications on developments in the HPOM area,<sup>[4-6]</sup> the role of the central template in these exceptionally stable molecules has primarily remained a structural one.<sup>[6]</sup>

[\*] Dr. D.-L. Long, H. Abbas, Dr. L. Cronin  
 Department of Chemistry  
 The University of Glasgow  
 Glasgow, G12 8QQ (UK)  
 Fax: (+44) 141-330-4888  
 E-mail: L.Cronin@chem.gla.ac.uk

Dr. P. Kögerler  
 Ames Laboratory and Department of Physics & Astronomy  
 Iowa State University  
 Ames, IA 50011 (USA)

[\*\*] This work was supported by the Leverhulme Trust (London), The Royal Society and The University of Glasgow. The EPSRC provided funds for the X-ray diffractometer. Ames Laboratory is operated for the U.S. Department of Energy by Iowa State University Contract No. W-7405-Eng-82.

Supporting information for this article is available on the WWW under <http://www.angewandte.org> or from the author.

One particularly interesting family of HPOMs is based on the very stable Dawson structural type ([M<sub>18</sub>O<sub>54</sub>(XO<sub>4</sub>)<sub>2</sub>]<sup>m-</sup>; M = Mo or W, X = main-group element) which contains two tetrahedral anions and a metal oxide framework structure (MO<sub>3</sub>)<sub>18</sub>. This class of HPOM cluster was first structurally characterized fifty years ago and since then the subject of many hundreds of papers.<sup>[2,7]</sup> We are interested in the design of new fundamental types of isopolyoxometalates<sup>[8,9]</sup> as well as non-conventional HPOM clusters<sup>[10]</sup> that incorporate two pyramidal anions,<sup>[11]</sup> similar to the Dawson archetype, as such clusters may exhibit unprecedented properties arising from the intramolecular electronic interactions between the encapsulated anions, thus providing a novel route to manipulate the physical properties of the {M<sub>18</sub>} Dawson-type clusters.

In an attempt to develop internally switchable molecular clusters based on polyoxometalates, we have recently discovered the sulfite-based Dawson-type polyoxomolybdates α- and β-[Mo<sup>VI</sup><sub>18</sub>O<sub>54</sub>(SO<sub>3</sub>)<sub>2</sub>]<sup>4-</sup> (**1a** and **1b**, respectively). They incorporate two adjacent sulfite anions in a configuration causing a short, yet non-bonding intramolecular S··S interaction between the sulfite anions and exhibit unusual reversible thermochromic properties over the temperature range 77 to 500 K.<sup>[10]</sup> In an extension of this work we succeeded in synthesizing the first two examples of polyoxotungstate clusters incorporating the sulfite anion,<sup>[12]</sup> [W<sup>VI</sup><sub>18</sub>O<sub>54</sub>(SO<sub>3</sub>)<sub>2</sub>]<sup>4-</sup> (**2a**), the isostructural tungstate analogue to **1a**, and [W<sup>VI</sup><sub>18</sub>O<sub>56</sub>(SO<sub>3</sub>)<sub>2</sub>(H<sub>2</sub>O)<sub>2</sub>]<sup>8-</sup> (**3a**; see Figure 1). They were isolated as (Bu<sub>4</sub>N)<sub>4</sub>[W<sup>VI</sup><sub>18</sub>O<sub>54</sub>(SO<sub>3</sub>)<sub>2</sub>] (**2**) and K<sub>7</sub>Na[W<sup>VI</sup><sub>18</sub>O<sub>56</sub>(SO<sub>3</sub>)<sub>2</sub>(H<sub>2</sub>O)<sub>2</sub>]·20H<sub>2</sub>O (**3**) and characterized by single crystal X-ray structure analysis,<sup>[13]</sup> elemental analysis, IR and UV-Vis spectroscopy, bond valence sum (BVS) and DFT calculations.<sup>[14]</sup>

Interestingly, **3a** has a curious structure including two terminal water ligands which is unknown for closed-shell HPOM clusters of any type.<sup>[15]</sup> Moreover, **3** also demonstrates unprecedented electronic properties: the cluster anion **3a**, [W<sub>18</sub>O<sub>56</sub>(SO<sub>3</sub>)<sub>2</sub>(H<sub>2</sub>O)<sub>2</sub>]<sup>8-</sup>, undergoes a unique electron-transfer reaction when heated, in which a structural re-arrangement allows the two embedded pyramidal sulfite (S<sup>IV</sup>O<sub>3</sub><sup>2-</sup>) anions to release up to four electrons (analogous to the “soldiers” hidden inside the “Trojan Horse”) to the surface of the cluster generating the sulfate-based, deep blue, mixed-valence cluster [W<sub>18</sub>O<sub>54</sub>(SO<sub>4</sub>)<sub>2</sub>]<sup>8-</sup>. Although electron-transfer reactions and structural rearrangements are very well known for HPOMs,<sup>[6]</sup> this is the first example of a coupled structural-rearrangement and electron-transfer process, whereby the electrons are “released” from the core of the cluster. It is also the first example of a fully characterized unimolecular reaction involving an HPOM.

To fully explore and understand these properties we must consider the structural differences between the cluster anions **2a** and **3a**. The structures of both clusters consist of two {W<sub>9</sub>(SO<sub>3</sub>)} halves which contain six equatorial and three capping metal positions. The two halves are joined by linking each of the six equatorial metal atoms of each half together through six bridging oxo ligands (Figure 1 and Figure 2). The key structural differences between these two cluster families are primarily based on the relative orientation of their two sulfite groups (Figure 2) whereby the base of the pyramid

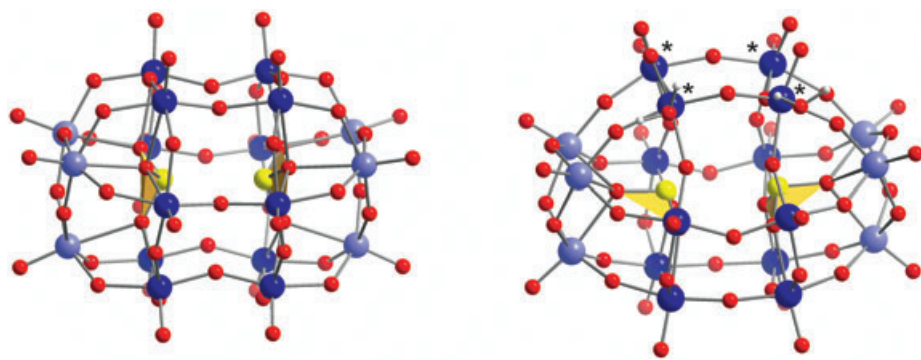


**Figure 1.** Ball-and-stick representations of the structures of the  $D_{3h}$ -symmetric  $\alpha$ -[W<sub>18</sub>O<sub>54</sub>(SO<sub>3</sub>)<sub>2</sub>]<sup>4-</sup> (**2a**, left) and the  $C_{2v}$ -symmetric [W<sub>18</sub>O<sub>56</sub>(SO<sub>3</sub>)<sub>2</sub>(H<sub>2</sub>O)<sub>2</sub>]<sup>8-</sup> (**3a**, right) cluster anions; light blue spheres represent capping {W<sub>3</sub>}, dark blue spheres represent equatorial {W<sub>6</sub>}, red O, gray H, yellow S. Yellow polyhedra represent the pyramidal SO<sub>3</sub> units and emphasize their different relative orientations within each framework; \* marks tungsten units that are not coordinated to the sulfite groups and thus have two terminal oxo ligands.

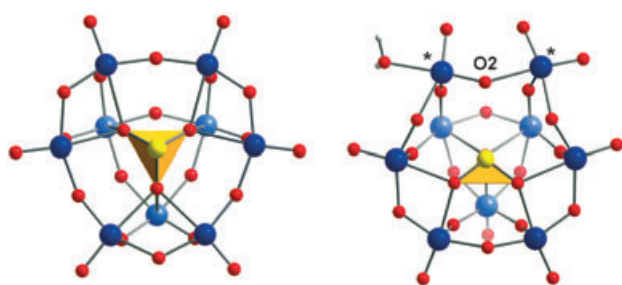


**Figure 2.** Schematic comparison of the SO<sub>3</sub> coordination mode in **2a** (left) and **3a** (right). Only one {W<sub>9</sub>(SO<sub>3</sub>)} half is shown, viewed along the long axis of the cluster. Colors are as in Figure 1.

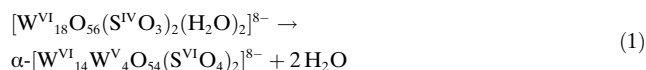
formed by the trigonal-pyramidal SO<sub>3</sub> group in **2a** is centrally aligned and binds to all nine metal centers of each {W<sub>9</sub>(SO<sub>3</sub>)} fragment, whereas in compound **3a** the SO<sub>3</sub> pyramids are tilted so that only seven of the nine metal centers of each {W<sub>9</sub>(SO<sub>3</sub>)} fragment are connected.

This arrangement leaves four neighboring equatorial tungsten positions in **3a** uncoordinated to the templating sulfite groups and thereby reduces the overall molecular symmetry from  $D_{3h}$  (**1a** and **2a**) to  $C_{2v}$  with the loss of a number of mirror planes and the  $C_3$  axis for **3a**. The significantly different orientations of the sulfite ions in **3a** compared to **1a** and **2a** is also reflected by the S⋯S distance of 3.61(2) Å in **3a** which is significantly longer than the distance of 3.19(1) Å in **2a** and 3.27(1) Å in **1a**.

The second major structural difference between **2a** and **3a** lies in the number of terminal oxo ligands present in each cluster type. All of the metal atoms present in **2a** (as well as in **1a**) only support one terminal oxo ligand that is not shared by other metal atoms, however cluster **3a** contains four tungsten units (labeled as W\* in Figures 1 and 2), each with two terminal ligands. This situation arises because these two tungsten units are not bonded to the embedded sulfite groups. The two terminal ligands and four bridging  $\mu_2$ -oxo (O<sup>2-</sup>) ligands per W\* center complete a slightly distorted octahedral coordination geometry. Structural analysis (including bond

valence sum analysis) reveals that while two of the four unique W\* centers each have two terminal oxo ligands (W=O ca. 1.7 Å), the other two W\* centers each have one terminal oxo ligand and one terminal water ligand (W=O ca. 1.7 Å and W–OH<sub>2</sub> ca. 2.2 Å). There is a slight disorder but the presence of two water ligands and two oxo ligands is confirmed by the average bond valence sums as well as chemical and thermal analysis. Furthermore the bridging oxo group (O2 in Figure 2) between the two W\* positions of a {W<sub>9</sub>(SO<sub>3</sub>)} half is now folded into the cluster and points towards the vacant site of the SO<sub>3</sub> pyramid with a O2⋯S distance of 2.96(2) Å, whereas the equivalent position in **1a** and **2a** points outwards.

The structure of **3a** is already pre-arranged for an internal reorganization and a concurrent internal redox reaction, in which the encapsulated sulfite anions act as embedded reducing agents, and are oxidized to sulfate when heated to over 400 °C. In the course of this reaction a maximum of four electrons could be transferred to the metal oxide framework, causing the color change from colorless ({W<sup>VI</sup><sub>18</sub>}) to blue ({W<sup>VI</sup><sub>14</sub>W<sup>V</sup><sub>4</sub>). The overall reaction is accompanied by the release of the two coordinated water ligands from the W\* centers. Because the reduction of the metal oxide shell by four electrons is balanced by the internal oxidation of the two sulfite anions (to sulfate groups), the overall charge of the cluster remains identical to give [W<sup>VI</sup><sub>14</sub>W<sup>V</sup><sub>4</sub>O<sub>54</sub>(SO<sub>4</sub>)<sub>2</sub>]<sup>8-</sup> (**4a**). The reaction can be summarized as shown in Equation (1).



This reaction mechanism is confirmed by a variety of experiments which includes the observation of the loss of two water molecules at 400 °C, indicated in the IR spectrum and quantified by thermogravimetric analysis (TGA). The formation of the two sulfate moieties is shown by the IR and Raman spectra (emergence of an additional band at 650 cm<sup>-1</sup>, attributed to sulfate) and in differential scanning calorimetry (DSC) traces, a sharp exothermic process associated with the onset of the internal redox reaction and the formation of sulfate at ca. 400 °C (Figure 3).

Analysis of compound **4** (K<sub>7</sub>Na[W<sub>18</sub>O<sub>54</sub>(SO<sub>4</sub>)<sub>2</sub>]) also confirms its formula, and the four-electron reduced polyoxotungstate shell which is also indicated by the transformation of colorless **3** into deep blue **4**. This data also confirms that **4a** is not protonated, which is confirmed by the loss of the H(-O) signal in solid-state <sup>1</sup>H magic angle spinning (MAS) NMR spectrum. Given the unambiguous analytical data for the formation of **4** it is unfortunate that crystals suitable for single-crystal X-ray diffraction could not be obtained and that it is exceptionally reactive, but **4** is stable for many weeks if sealed in an evacuated glass tube. However, we are able to confidently suggest that the mixed-valence framework of the

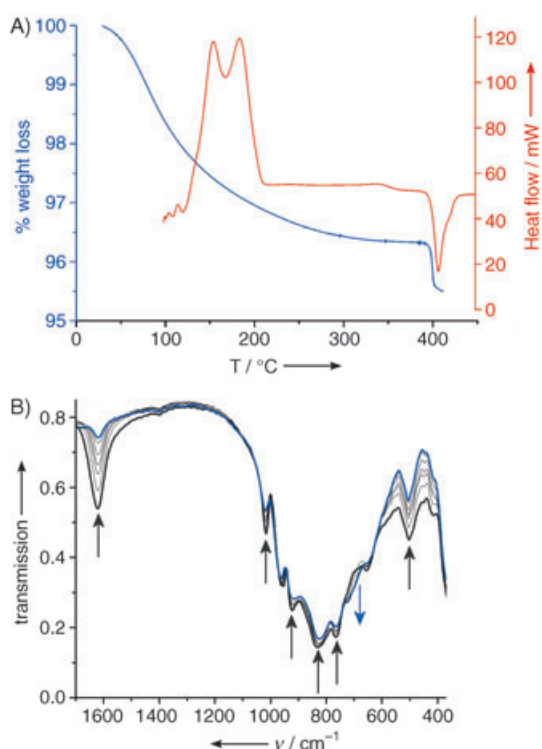


**Figure 3.** A) TGA (blue line) and DSC (red line) results. B) the IR spectrum of **3** (dark gray line) and the product **4** (blue line). Arrows indicate the changes going from **3** to **4**. The weight loss of just under 0.9% at 400°C correlates with the loss of two water molecules. The exothermic peak in the DSC curve at 400°C is consistent with the formation of the sulfate groups.

product  $\alpha$ -[W<sub>18</sub>O<sub>54</sub>(SO<sub>4</sub>)<sub>2</sub>]<sup>8-</sup> (**4a**) is equivalent to the fully oxidized framework of the conventional sulfate-based Dawson cluster  $\alpha$ -[W<sub>18</sub>O<sub>54</sub>(SO<sub>4</sub>)<sub>2</sub>]<sup>4-</sup> (**5a**), which can be synthesized by the reaction of tungstate in the presence of sulfate anions.<sup>[16]</sup> This structural hypothesis follows from a comparison of the structure of the cluster anion **5a** with that of the starting species **3a**. Overlaying the two structures reveals that the positions of all the tungsten and sulfur centers are identical to within 0.30(2) Å. We therefore hypothesize that the frameworks of the reduced product **4a** and oxidized **5a** are virtually isostructural; this idea is also supported by the fact that almost all other {M<sub>18</sub>} clusters with tetrahedral templates (over 80 are reported) display the same metal oxide framework geometry and may only differ in the relative orientation of the capping {M<sub>3</sub>} units giving several isomeric possibilities.

To examine this hypothesis, the preliminary energetic features of a pathway for the reaction in Equation (1) can be established from ab initio density functional theory (DFT) calculations.<sup>[14]</sup> Owing to the complexity of the system, the complete energy hyper-surface cannot be obtained and we thus used an approximate transition state. This transition-state geometry was obtained from geometrical arguments by interpolation between the atomic coordinates in **3a** and **5a**. Although the results can only be interpreted semi-quantitatively, they agree with the existence of a substantial activation barrier requiring heating and a subsequent exothermic step.

The energy difference between **3a** and the transition state (plus two water molecules), that is, the reaction state representing the thermodynamic barrier, is approximately 200 kJ mol<sup>-1</sup>, while the step from the transition state to the final state is characterized by an energy gain of approximately 450 kJ mol<sup>-1</sup>, rendering the final state (**4a** + 2H<sub>2</sub>O) around 250 kJ mol<sup>-1</sup> more stable than **3a**. The energy release during the exothermic process at 400°C (when **3** transforms to **4**) measured using DSC (288 kJ mol<sup>-1</sup>) coincides within 15% with the theoretical result. This comparison therefore provides a striking link between theory and experiment.<sup>[17]</sup> The initial step of the reaction in Equation (1) requires movement of some of the terminal and bridging oxygen ligands of the W1 and W2 centers (Figure 4). First, the O1, O2 (both blue) and the O3, O4 (orange) positions shown in Figure 4A and 4B rotate clockwise about the central tungsten atoms through the transition state (Figure 4A, center) until the terminal O1 (bound to W1) position is within bonding distance of W2 and

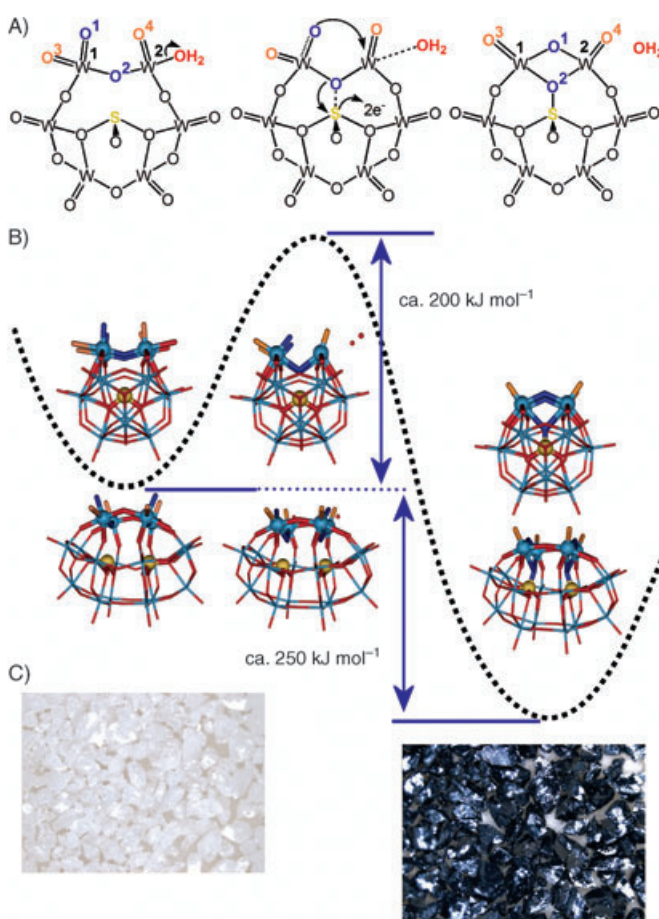


**Figure 4.** A) Scheme illustrating the proposed reaction mechanism. For clarity only the equatorial cluster “belts” and the central sulfur position of a {W<sub>9</sub>(SO<sub>3</sub>)} fragment are shown. B) The structures of the cluster reactant **3a**, the transition state, and the product **4a** are shown and are superimposed on the suggested energy pathway (both a top view and side view of the clusters are shown for clarity with the red O, light blue W, yellow S). A common color scheme is used in (A) and (B) for the oxygen atoms that move during the transformation. C) Photographs of the crystals of the reactant **3** (colorless; left) and the product **4** (blue; right).

the bridging O2 center moving towards the sulfur atom reaches bonding distance with this center.

As can be seen in Figure 4A and 4B, the oxygen trajectories during the transformation are extremely ( $O1 \Delta = 1.8 \text{ \AA}; 66^\circ$ ), ( $O2 \Delta = 1.5 \text{ \AA}; 37^\circ$ ), ( $O3 \Delta = 1.2 \text{ \AA}; 30^\circ$ ), ( $O4 \Delta = 1.2 \text{ \AA}; 37^\circ$ ). Finally, as the bond is being made between O1 and W2 the *trans*-positioned water ligand on W2 is cleaved off (an animation of this transformation, generated by the interpolation of the coordinates between **3a** and **5a**, is present in the Supporting Information).

In conclusion, the enclosure of sulfite anions with a "correct" orientation in an HPOM cluster shell transforms these anions from "innocent" structural templates to electronically reactive, functional units. The sulfite ions can now release electrons to the cluster shell upon activation by heat (the sulfite groups in cluster **3a** are "activated" whereas those in **2a** are not). Therefore this new class of "activated" metal oxide cluster shows promise for the development of novel functional metal oxides, and **3a** is the first characterized inorganic cluster to undergo a concerted reaction in which a unimolecular process is characterized by a coupled structural and electronic rearrangement. Although the transformation of **3** to **4** does not appear reversible we will seek to extend this system, for example, by the replacement of the water groups for other ligands.

## Experimental Section

**2**:  $\text{Na}_2\text{WO}_4 \cdot 2\text{H}_2\text{O}$  (6.6 g, 20 mmol) and  $\text{Na}_2\text{SO}_3$  (2.4 g, 19 mmol) were dissolved in water (25 mL). Hydrochloric acid (37%, 5 mL) was added to the stirred solution and the pH value of the solution was adjusted to 1.9 using diluted hydrochloric acid. The solution was then heated under reflux for 72 h. After cooling, the solution was added to a solution of  $\text{Bu}_4\text{NBr}$  (6.0 g, 18.6 mmol) in water (200 mL). A white precipitate was collected by centrifuging, washed with water and ethanol, and dried in vacuum. Recrystallization of the solid in acetonitrile afforded cream yellow crystals of **2** (yield 2.3 g, 39%). IR (KBr disk):  $\tilde{\nu} = 3434, 2961, 2873, 1625, 1482, 1379, 1151, 1105, 993, 915, 877, 779 \text{ cm}^{-1}$ ; elemental analysis (%) calcd for  $\text{C}_{64}\text{H}_{144}\text{W}_{18}\text{N}_4\text{O}_{60}\text{S}_2$ : C 14.5, H 2.7, N 1.1, W 62.4; found: C 14.2, H 2.6, N 1.2, W 63.0.

**3**: Compound **3** was produced in the same procedure as **2** except that in the final step solid KCl (5.0 g, 67 mmol) was added to the reaction mixture instead of a  $\text{Bu}_4\text{NBr}$  solution and the mixture was stirred for 2 h to yield a white precipitate, which was collected and then recrystallized in minimum water (ca. 140 mL) with the addition of KCl (2 g) and drops of diluted hydrochloric acid to keep the pH value at 2.0. After the solution was concentrated to about 100 mL (by evaporation in air), the colorless crystals of **3** were collected (yield 2.3 g, 41%). IR (KBr disk):  $\tilde{\nu} = 3434, 1623, 1017, 917, 800 \text{ cm}^{-1}$ ; elemental analysis (%) calcd for  $\text{H}_{44}\text{K}_7\text{NaO}_{84}\text{S}_2\text{W}_{18}$ : K 5.4, Na 0.45, W 65.4%; found: K 4.8, Na 0.40, W 66.1. The purity of the bulk phases was confirmed by powder diffraction.

Received: February 14, 2005

Published online: May 4, 2005

**Keywords:** electron transfer · polyoxometalates · rearrangement · sulfur · tungsten

- [1] A. Müller, S. Roy, *Coord. Chem. Rev.* **2003**, *245*, 153; A. Müller, P. Kögerler, C. Kuhlmann, *Chem. Commun.* **1999**, 1347.
- [2] P. J. S. Richardt, R. W. Gable, A. M. Bond, A. G. Wedd, *Inorg. Chem.* **2001**, *40*, 703; T. Ruther, V. M. Hultgren, B. P. Timko, A. M. Bond, W. R. Jackson, A. G. Wedd, *J. Am. Chem. Soc.* **2003**, *125*, 10133.
- [3] W. B. Kim, T. Voitl, G. J. Rodriguez-Rivera, S. T. Evans, J. A. Dumesic, *Angew. Chem.* **2005**, *117*, 788; *Angew. Chem. Int. Ed.* **2005**, *44*, 778.
- [4] T. M. Anderson, W. A. Neiwert, M. L. Kirk, P. M. B. Piccoli, A. J. Schultz, T. F. Koetzle, D. G. Musaev, K. Morokuma, R. Cao, C. L. Hill, *Science* **2004**, *306*, 2074.
- [5] *Polyoxometalate Chemistry: from Topology via Self-assembly to Applications* (Eds.: M. T. Pope, A. Müller), Kluwer: Dordrecht, **2001**, pp. 1–467; K. Wassermann, M. H. Dickman, M. T. Pope, *Angew. Chem.* **1997**, *109*, 2552; *Angew. Chem. Int. Ed. Engl.* **1997**, *36*, 1445.
- [6] T. Yamase, *Chem. Rev.* **1998**, *98*, 307; F. Hussain, B. S. Bassil, L.-H. Bi, M. Reicke, U. Kortz, *Angew. Chem.* **2004**, *116*, 3567; *Angew. Chem. Int. Ed.* **2004**, *43*, 3485.
- [7] B. Dawson, *Acta Crystallogr.* **1953**, *6*, 113; M. Holscher, U. Englert, B. Zibrowius, W. F. Holderich, *Angew. Chem.* **1994**, *106*, 2552; *Angew. Chem. Int. Ed. Engl.* **1994**, *33*, 2491.
- [8] D.-L. Long, P. Kögerler, L. J. Farrugia, L. Cronin, *Angew. Chem.* **2003**, *115*, 4312; *Angew. Chem. Int. Ed.* **2003**, *42*, 4180.
- [9] D.-L. Long, H. Abbas, P. Kögerler, L. Cronin, *J. Am. Chem. Soc.* **2004**, *126*, 13880.
- [10] D.-L. Long, P. Kögerler, L. Cronin, *Angew. Chem.* **2004**, *116*, 1853; *Angew. Chem. Int. Ed.* **2004**, *43*, 1817.
- [11] Surprisingly, there are few examples of  $[\text{M}_{18}]$  Dawson-like clusters that host non-tetrahedral anions, presumably due to size restrictions, examples include a single pyramidal anion ( $[\text{BiO}_3]^{3-}$  or  $[\text{AsO}_3]^{3-}$ ) in each cluster (see Y. Ozawa, Y. Sasaki, *Chem. Lett.* **1987**, 923 and Y. Jeannin, J. Martin-Frere, *Inorg. Chem.* **1979**, *18*, 3010) or a di-tetrahedral anion ( $[\text{P}_2\text{O}_7]^{4-}$ , two  $\text{PO}_4$  tetrahedra sharing one corner, see S. Himeno, A. Saito, T. Hori, *Bull. Chem. Soc. Jpn.* **1990**, *63*, 1602 and U. Kortz, M. T. Pope, *Inorg. Chem.* **1994**, *33*, 5643).
- [12] The compounds reported herein are the first examples of tungstosulfites and it should be noted that structurally characterized molybdosulfites are also rare, in addition to reference [10] see: M. J. Manos, J. D. Woollins, A. M. Z. Slawin, T. A. Kabanos, *Angew. Chem.* **2002**, *114*, 2925; *Angew. Chem. Int. Ed.* **2002**, *41*, 2801, and references therein.
- [13] Crystal data and structure refinements for **2**:  $\text{C}_{64}\text{H}_{144}\text{N}_4\text{O}_{60}\text{S}_2\text{W}_{18}$   $M_r = 5303.25 \text{ g mol}^{-1}$ ; a block crystal ( $0.24 \times 0.14 \times 0.08 \text{ mm}^3$ ) was analyzed with a Kappa CCD diffractometer using  $\text{MoK}\alpha$  radiation ( $\lambda = 0.71073 \text{ \AA}$ ) at 150(2) K. Orthorhombic, space group  $Pnn2$ ,  $a = 26.7514(5)$ ,  $b = 28.5677(5)$ ,  $c = 15.7284(2) \text{ \AA}$ ,  $V = 12020.1(3) \text{ \AA}^3$ ,  $Z = 4$ ,  $\rho = 2.931 \text{ g cm}^{-3}$ ,  $\mu(\text{MoK}\alpha) = 17.26 \text{ mm}^{-1}$ ,  $F(000) = 9600$ , 44592 reflections measured, of which 21004 are independent, 1228 refined parameters,  $R1 = 0.0371$ ,  $wR2 = 0.0766$ . **3**:  $\text{H}_{44}\text{K}_7\text{NaO}_{84}\text{S}_2\text{W}_{18}$ ,  $M_r = 5058.46 \text{ g mol}^{-1}$ ; block crystal:  $0.16 \times 0.10 \times 0.05 \text{ mm}^3$ ;  $T = 120(2) \text{ K}$ . Monoclinic, space group  $P2_1/c$ ,  $a = 22.2248(4)$ ,  $b = 12.6847(2)$ ,  $c = 28.2393(5) \text{ \AA}$ ,  $\beta = 96.0234(7)^\circ$ ,  $V = 7817.1(2) \text{ \AA}^3$ ,  $Z = 4$ ,  $\rho = 4.244 \text{ g cm}^{-3}$ ,  $\mu(\text{MoK}\alpha) = 26.58 \text{ mm}^{-1}$ ,  $F(000) = 8896$ , 65801 reflections measured, of which 15487 are independent, 1078 refined parameters,  $R1 = 0.0562$ ,  $wR2 = 0.1202$ . CCDC 249657 and CSD 414366 contain the supplementary crystallographic data for this paper. These data can be obtained free of charge from the Cambridge Crystallographic Data Centre via [www.ccdc.cam.ac.uk/data\\_request/cif](http://www.ccdc.cam.ac.uk/data_request/cif).
- [14] Computation details: Density functional theory calculations (including Löwdin and Mulliken population analysis) using the TURBOMOLE 5.6 package required TZVPP basis sets and

hybrid B3-LYP exchange-correlation functionals to converge. All structures ( $C_1$  symmetry) were allowed to briefly equilibrate until a small, consistent mean energy gradient  $|dE/dxyz|$  was reached. The mean shift for each atomic position generated by the free geometric equilibration amounted to 0.007 Å. Initial structures for the starting and the final reagent were obtained from crystallographic data for **3** and **5**, respectively, with two water molecules added to the final geometry.

- [15] This is, to our knowledge, the first example of a non-lacunary HPOM which includes tungsten centers with more than one terminal ligand.
- [16] S. Himeno, H. Tatewaki, M. Hashimoto, *Bull. Chem. Soc. Jpn.* **2001**, *74*, 1623.
- [17] Other characteristic electronic properties support the suggested reaction pathway as well: A gradual transfer of charge density from the sulfite groups in the initial state **3a** to the tungsten positions in the final state is reflected by a continuous decrease in the HOMO–LUMO energy gap and a gradual decrease of the tungsten partial atomic net charges. In the final product, the four electrons are delocalized over all 18 tungsten positions, resulting in nearly uniform Löwdin partial charges (with standard deviations of 2%). Throughout the series, the Löwdin charges of the sulfur positions successively increase from 0.173 (**3a**) to 0.186 (transition state) to 0.198 (final product), a pattern corresponding to the oxidation of the sulfite groups.